

# Nature and causes of flow-induced noise on a sonar with a towed triplet array receiver

S P Beerens and S P van IJsselmuide

Netherlands Organisation for Applied Scientific Research (TNO),  
Physics and Electronics Laboratory (FEL),  
PO Box 96864, 2509 JG The Hague.  
E-mail: Beerens@fel.tno.nl

## Abstract

In the design of towed array sonar receivers the reduction of flow-induced noise is an important issue. In this paper theory on flow noise and several methods to analyse flow noise are presented. These methods are applied to sea trial data of an experimental triplet array. The obtained results agree well with accepted theory. It appears that the methods in combination provide not only the levels, but also the causes of flow noise.

## 1 Introduction

In modern Anti Submarine Warfare (ASW) towed linear antennas are used to receive acoustic signals, which have been emitted or reflected from targets underwater. In such antennas, referred to as towed arrays, hydrophones are spaced equidistantly. The advantage of towed arrays is that they have the possibility to determine accurately the direction of arrival of the received signals, associated with signal processing gain. Furthermore towed arrays can be operated at the most profitable depth, in contrary to classical hull-mounted sonars.

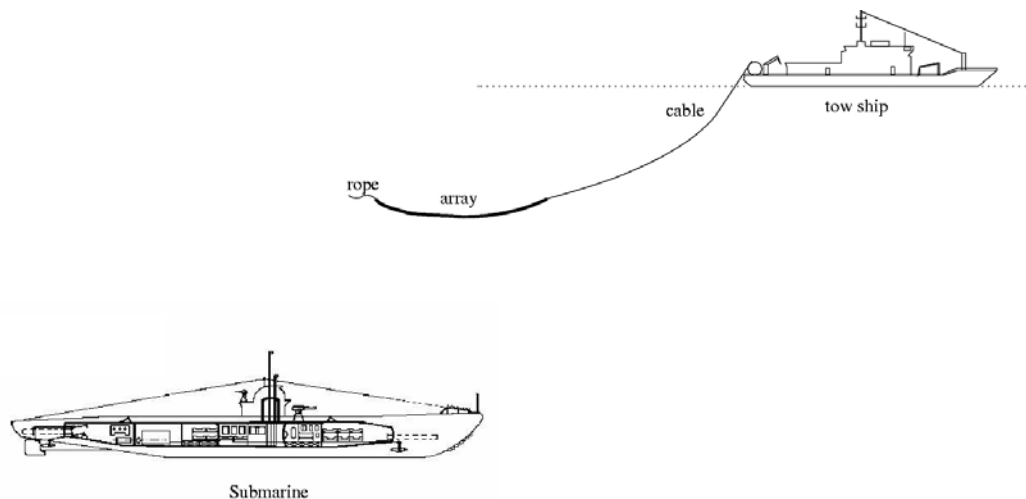


Figure 1 Schematic ASW scenario

In the design of new types of towed arrays self noise is an important issue. Self noise is generated by the sonar system itself, mainly caused by towing the sonar through the water. This paper focuses on the main cause of self noise, named hydrodynamic noise, or more commonly *flow noise*. It may be clear that flow noise should never be limiting the performance of a sonar. Therefore it is necessary to determine the sources and levels of flow noise of a newly designed array and to compare these to other types of noise, such as sea noise. An overview of flow noise theory and data analysis techniques is presented in this paper, as well as an application to an experimental triplet array; see *Figure 2*.

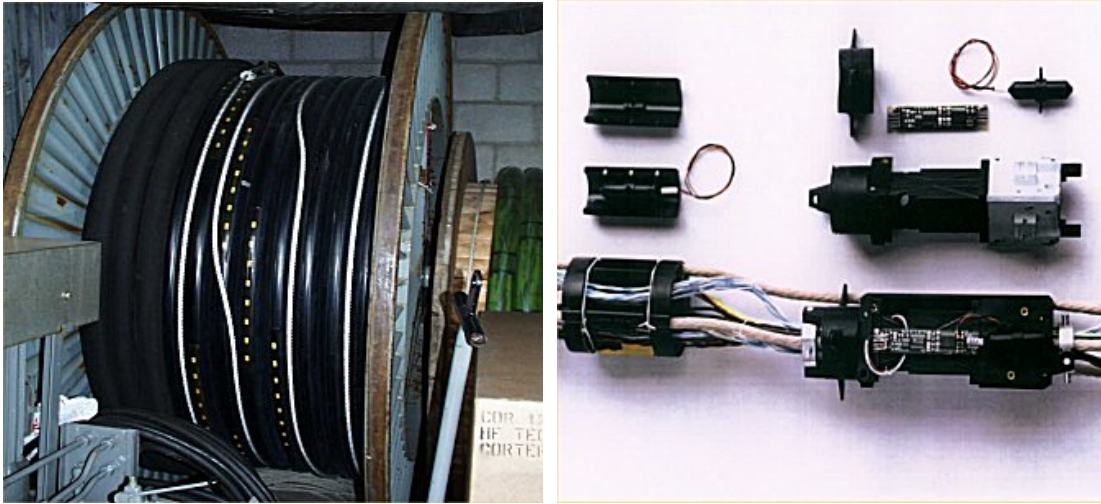


Figure 2 The TNO-FEL CAPTAS triplet array on a winch (left) and components (right).

The array in this application is the TNO-FEL CAPTAS (for Combined Active and Passive Towed Array Sonar) triplet array. This is an experimental array designed for ASW purposes. The use of *hydrophone triplets* in a single hosed towed array makes this array very suitable for shallow water application. It is easy to handle compared to multiple-array systems and still provides the ability to perform direct port-starboard discrimination; see [1]. A possible drawback from the use of triplets is that the processing is sensitive to uncorrelated noise and levels of flow noise maybe high as the hydrophones are positioned close to the hose wall [2].

An important issue in the design of triplet arrays is to know how much its diameter can be reduced with respect to the acoustic wavelength, and for a given hose diameter, to know what is the best internal position for the hydrophones. For this issue, the knowledge of flow noise levels and correlation characteristics is essential.

In this paper the levels and causes of flow noise are studied at different tow speeds. Flow noise data of the triplet array are analysed with several techniques. The data have been obtained in sea trials directed by TNO-FEL in the Mediterranean in 1997.

The paper is organised as follows. In Chapter 2 a detailed theoretical overview of all flow noise contributions is given. The experiment set-up for the triplet array is described in Chapter 3. It appears that in practice it is hard to recognise the flow noise contributions in experimental data, which also contains other types of noise. Hence, the noise spectrum of a single hydrophone (as worked out in Chapter 4) does not reveal the relative importance of the various noise-producing mechanisms. However, since a linear hydrophone array provides us with information on the spatial distribution of the noise field, signal processing tools can help us to isolate the different noise contributions. In Chapter 5 a relatively simple tool, coherence analysis, is successfully applied to distinguish between the different noise contributions. In Chapter 6 a more sophisticated tool, i.e. wavenumber-frequency ( $k-\omega$ ) analysis, is applied to the same problem. This leads to conclusions in Chapter 7.

The research in this paper is performed in the framework of the New Array Technology (NAT) programme. This programme aims at developing new technologies for low frequency active towed array sonars in shallow waters. In modern anti-submarine warfare shallow waters have become of increasing interest. For sonar applications shallow waters have specific problems and therefore TNO-FEL has initiated a co-operative research programme in this field together with the French sonar manufacturer Thales Underwater Systems SAS. The NAT programme is sponsored by the Dutch and the French MoD.

## 2 Flow noise theory

There are different ways in which the water flow along a towed array contributes to the noise (pressure fluctuations) received on the hydrophones, see e.g.

[3]. A distinction is made between the flow-induced excitation of *vibrations in the array* and the effect of the turbulent boundary layer (TBL) near the hose wall, which creates *turbulence-induced noise* on the hydrophones. Both effects induce pressure fluctuations, which are not true sound (sound is a longitudinal pressure wave), but do influence hydrophone output. Therefore the term “pseudo-sound” is often used for these effects.

### 2.1 Vibrations in the array

The tow cable is pulled through the water at a certain angle w.r.t. the direction of motion. Vortex shedding from the cable causes cable vibrations, or *cable strumming*. This results in a vibrating force on the towed array. In the same way hydrodynamic instability at the end of the array causes the tail to vibrate, so called *tail wagging*. These vibrations are damped by Vibration Isolation Modules (VIMs), but this damping is generally insufficient. Both cable strumming and tail wagging cause vibrations in the towed array, which induce three types of propagating waves:

1. breathing waves in the fluid filled hose,
2. extensional waves in the hose wall,
3. resonances and other very long waves.

#### Ad 1: breathing waves

Breathing waves are the main source of vibrational flow noise in towed arrays. These are pressure waves in the system of the incompressible fill fluid and the compliant hose wall, where the hose cross-section expands and contracts with over- and under-pressures in the fluid. The speed of breathing waves is in the order of 20 to 150 m/s for typical array constructions. Breathing waves are so dangerous because they travel in the fill fluid and therefore directly act on the hydrophones.

#### Ad 2: extensional waves in the hose wall

Extensional waves are elastic waves in the hose walls. The extensional wave speed depends on the hose wall material and is in the order of 100-500 m/s. Extensional wavelengths often exceed the length of an acoustic module. Such long waves cause pressure fluctuations in the fill fluid via Poisson coupling of longitudinal to radial displacement.

#### Ad 3: resonances

Still longer waves travel in the strength members or in the electronics of the array. These waves are so much longer than the acoustic module, that it looks as if all hydrophones are vibrating in a coherent way. These vibrations are grouped together under the name resonances.

The array vibrations may contribute significantly to flow noise, especially at low (passive) frequencies. Generally an  $f^{-4}$  law is proposed for vibrations, which does not mean that at higher (active) frequencies vibrations have no contribution. This occurs indirectly by means of *scattering mechanisms*. These mechanisms transfer the energy at low frequencies to higher (active) frequencies. The vibrational energy propagates along the array (with relatively high speed and low impedance) in longitudinal waves in hose wall and strength members. An object that is attached to the hose wall and/or the strength members is forced into vibration (with high impedance). These objects absorb energy of the breathing wave frequency to transmit this energy again in a much wider spectrum. To avoid this, vibrations should be damped as much as possible with VIMs and good care must be taken for the positioning of objects in the array.

## 2.2 Turbulence-induced noise

In addition to the effects of vibrations of the array, the direct transmission of the pressure fluctuations, of the Turbulent Boundary Layer (TBL) along the acoustic modules, into the fill fluid constitutes an important flow noise mechanism.

The first successful model for pressure fluctuations in the TBL was derived in the sixties by Corcos; see [4] and references therein. In the TBL, turbulent eddies cause local velocity fluctuations, which on their turn cause local pressure fluctuations at the hose wall. The frequency of these pressure fluctuations is related to the size of the eddies that are formed in the boundary layer. The speed,  $u$ , at which the eddies are carried downstream ('advected') is about 90% of the tow speed  $U$ :  $u \approx 0.9 U$ .

Most energy of the TBL pressure fluctuations appears to be concentrated at the low frequencies. Here the TBL energy spectrum is flat. The maximum frequency for which the spectrum remains flat, the so-called *break off frequency*, is related to a wavelength of about a fifth (empirical value) of the TBL-width  $\delta$ , see e.g.

[3]:

$$f_b = 5 u / \delta,$$

which is, depending on tow speed, in between 200 - 300 Hz for the triplet array; see Chapter 4. Below  $f_b$  the turbulent spectrum is flat and above  $f_b$  the spectral energy decays rapidly with  $f^{-3}$  according to Kraichnan turbulence theory; see *Figure 3*.

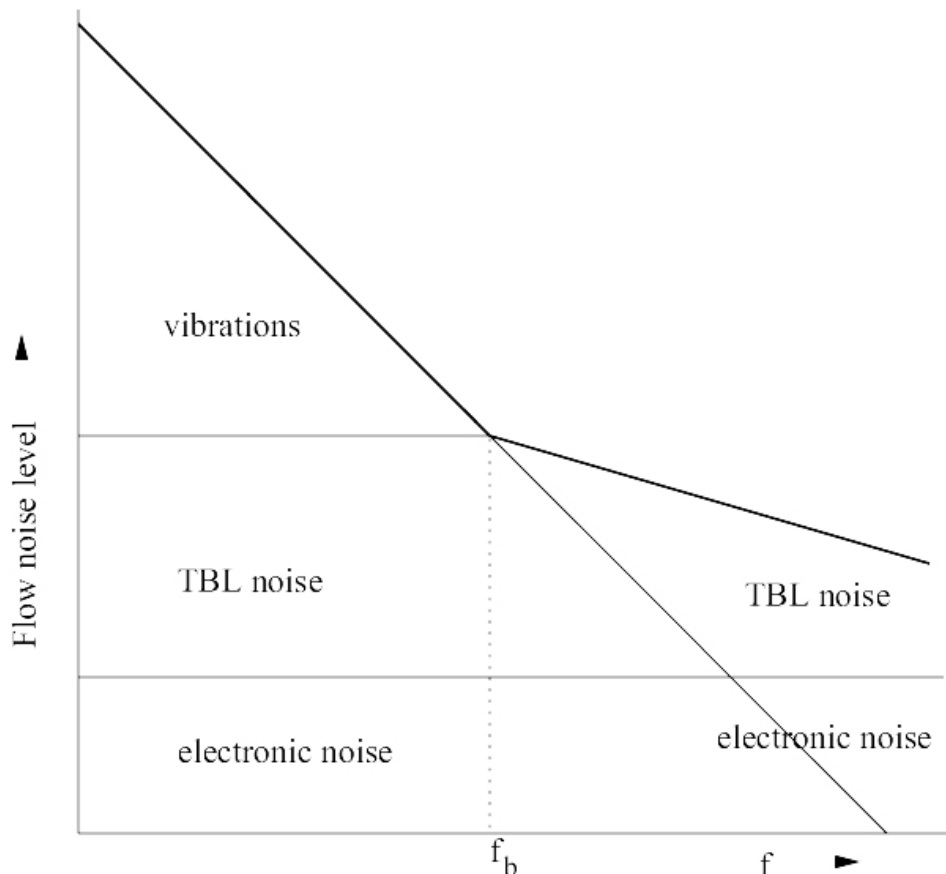


Figure 3 Spectrum of flow noise

In the discussion on received flow noise on hydrophones it is not only important to know how much flow noise an array produces, but also how sensitive the hydrophones are to the flow noise.

Therefore it is interesting to look at the spatial coherence scales in the TBL. It appears that correlation coefficients of pressure fluctuation in the TBL drop over very short length scales. Here we have to distinguish between the longitudinal and transverse direction

$$C_l(x) = \exp(-f/U x) \quad \text{and} \quad C_t(d) = \exp(-8f/U d).$$

For the latter it results that pressure fluctuations at the hose surface are correlated on a very short scale in the transverse direction. This means that the turbulent noise received on different hydrophones of the same triplet is probably not fully correlated, but to an extent, which depends both on turbulence spectrum and on hose elastic characteristics. The hose wall acts as a low pass filter upon TBL noise, modifying both energy and correlation of pressure fluctuations. The attenuation may be very severe; for  $f > 2 f_b$  it may be as much as -30 dB.

### 2.3 Discussion

The different sources of self noise in towed arrays are summarised in *Figure 4*. On the right hand side the vibrations caused by unstable towing are shown. These are mainly very low frequent and can be damped by a stabilising towed body and VIMs. They propagate as waves through the array and contribute to flow noise mostly indirectly.

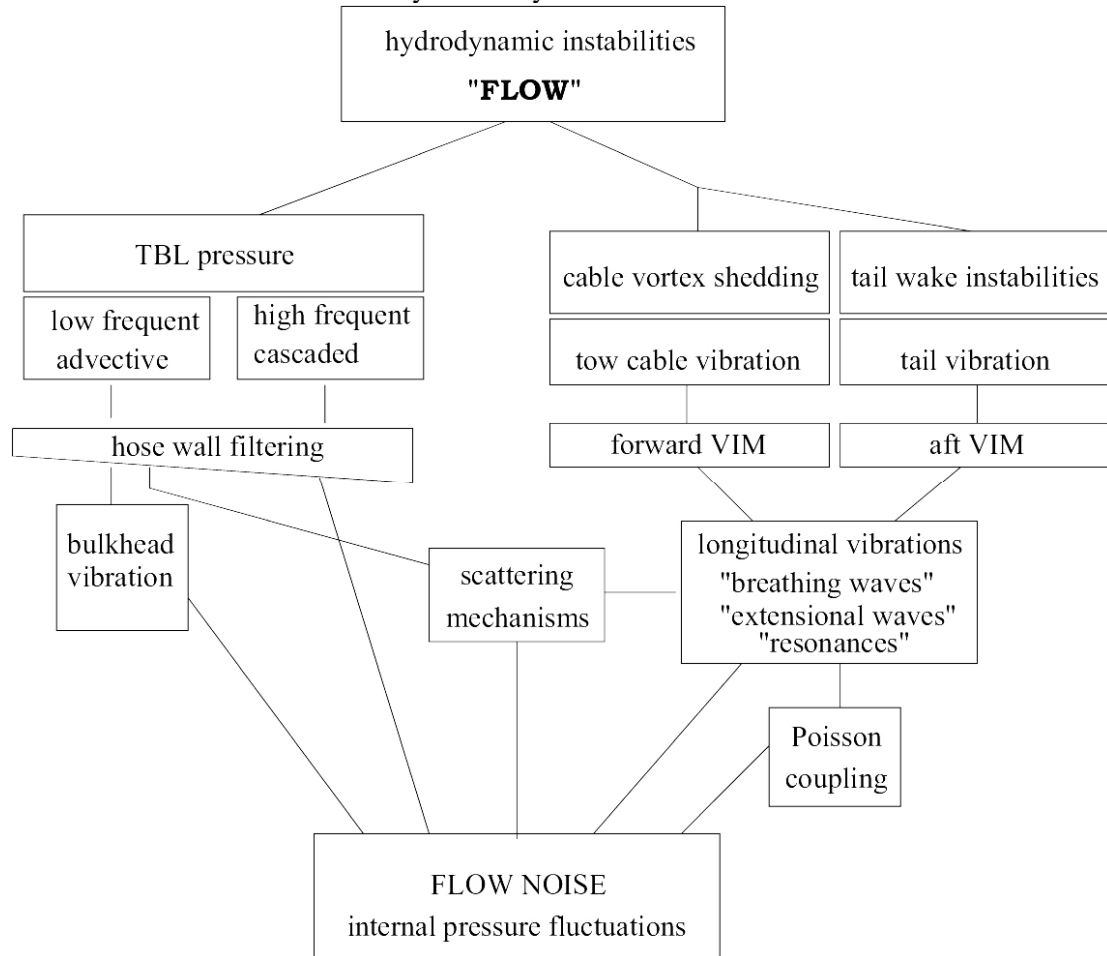


*Figure 4* Flow noise schematic

On the left hand side are shown turbulent pressure fluctuations. The low frequent TBL energy which enters the hose can easily be scattered and thereby be transferred to higher frequencies. This may especially occur near bulkheads or electronic equipment. High frequent TBL energy appears after energy cascades (break-up of eddies), but this energy is mostly filtered by the hose wall.

The conclusion from this theoretical study is that flow noise in towed arrays may be limiting in passive performance, but is not likely to be limiting in active performance, since flow noise levels drop off rapidly with frequency. In the next chapters we will show experimental results from the triplet array.

### 3 Triplet array experiments

The experimental triplet array used in this study consists of an acoustic section in between a front and an aft VIM. The acoustic section consists of 32 hydrophone triplets. The inter triplet spacing is 0.36 m or  $\lambda/2$  for 2070 Hz. The 3 hydrophones of each triplet are positioned on circle and fitted in a hose with external diameter of 85 mm. Flow noise experiments have been performed by TNO-FEL with this array in 1997 in the Mediterranean. In these experiments the triplet array is towed behind HNLMS Tydeman, the oceanographic research vessel that was kindly made available for this trial by the Royal Netherlands Navy; see *Figure 5*. Records have been made of flow noise experiments at four different speeds; 15, 12, 9 and 6 kts, respectively. Sea state, a measure for the background noise, increased during the experiments from 1 to 2. A long cable scope (1000 m) was used to minimise tow ship noise. The flow noise experiments with the triplet array in 1997 have been very successful. They provide a valuable, good quality data set. Analysis results show good agreement with accepted theory.



*Figure 5* HNLMS Tydeman the oceanographic research vessel of the Royal Netherlands Navy

### 4 Spectral analysis

Measured single hydrophone (array averaged) total noise spectra of the flow noise experiments are depicted in *Figure 3a*. The first thing that strikes are the high noise levels at low frequencies ( $< 100$  Hz). From the increase of these levels with tow speeds it is clear that this is dominated by flow noise (mainly vibrational). Turbulent flow noise becomes dominant only after the break-off frequency, which is dependent on tow speed somewhere in between 200-300 Hz. This corresponds well to the theoretical value:  $f = 5u/\delta$ . After this break off frequency the levels drop with about 25 dB per decade which is in between the theoretical value for flow noise (30 dB) and the value for sea noise (17 dB); see e.g. [5]. This behaviour is disturbed by some tonals of the tow ship. At active frequencies ( $> 1$  kHz) the importance of flow noise decreases rapidly. This shows up in the fact that the curves for the different tow speeds come closer together.

Although analysis of total noise spectra at different speeds is a standard method to study noise behaviour, it should be stressed that flow noise information is not easily derived from this approach. There are two error sources related to other noise contributions. A systematic error is caused by the fact that increasing the tow speed enhances tow ship noise, which leads to over-estimations of the flow noise level. Other errors occur by the fluctuating sea noise during the different experiments and the changing propagation conditions for the different tow depths.

Since the flow noise levels are only marginal, a slight increase of sea state or tow depth may disturb this approach. This is evident from *Figure 6a*, where the decreasing tow speed in the 6 kts experiment is fully compensated by an only slightly increased sea state (1  $\rightarrow$  2). In the next two chapters these problems are solved by more sophisticated analysis tools. These methods use the spatial structure of the noise field, which enables the separation of the different noise contributions to determine the flow noise levels very accurately.

*a*

*b*

*c*

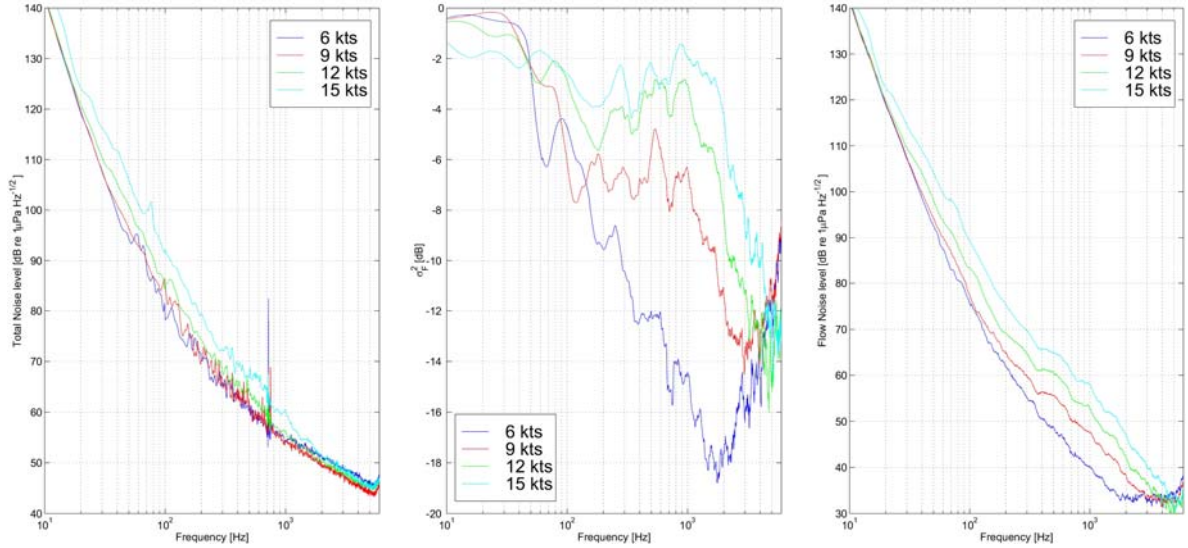


Figure 6 Spectra of Total noise ( a ), Ratio of flow noise to total noise ( b ) and Flow noise ( c ).

## 5 Coherence analysis

A very efficient way to separate the different noise contributions is coherence analysis; see e.g. [1]. This method makes use of the different spatial coherence (correlation) of the different noise contributions within a triplet. Noise can be subdivided into spatially correlated noise (mainly sea noise and tow ship noise) and spatially uncorrelated (mainly electronic and flow noise). The idea behind coherence analysis is that different noise types have different spatial coherence (correlation) and can be recognised by correlation measurements. To do so the theoretical spatial correlation functions of the noise compounds have to be known:

- Sea noise:  $C_S = \sin(kd) / kd$
- Flow noise:  $C_F = \exp(-8kd)$

with  $k = 2\pi f/c$  the acoustic wavenumber.

The condition for a proper separation of the mixture is that the correlation coefficients are far enough apart, preferably  $C_S \approx 1$  and  $C_F \approx 0$ . This condition is fulfilled if the hydrophones are close compared to the acoustic wavelength. This is generally only the case for low frequencies, but the triplet array with its intimate hydrophones inside the triplets does allow for coherence analysis at all interesting frequencies [1]. Inside triplets sea noise (and tow ship noise) is almost fully correlated.

Coherence analysis can mathematically be described by the following equations. The total noise power can be written as a sum of two parts,  $N_N^2 = N_S^2 + N_F^2$ , or equivalently in terms of noise ratios

$$1 = N_S^2 / N_N^2 + N_F^2 / N_N^2 = \sigma_S^2 + \sigma_F^2$$

The measured noise correlation coefficient between a pair of hydrophones separated by a distance  $d$  at a wavenumber  $k$  can be expressed as

$$C = \sigma_S^2 C_S + \sigma_F^2 C_F$$

If we measure hydrophone pair correlation coefficients ( $C$ ) we can solve the two noise ratios ( $\sigma^2$ ) from the above two equations (provided that the theoretical correlation functions are sufficiently accurate). This provides us with the ratio of flow noise to total noise ( $\sigma_F^2 = N_F^2 / N_N^2$ ), from which the flow noise levels ( $10^{10} \log N_F^2$ ) can be derived.

Now *coherence analysis* is applied to sea trial data to determine the flow noise levels. In *Figure 3a* the total noise spectra of the triplet array for 6, 9, 12 and 15 kts are depicted. The inner triplet correlation coefficients are determined and by means of coherence analysis the flow noise levels can be determined from these coefficients. The ratio of flow noise to total noise in dB is depicted in *Figure 3b*. At low frequencies (near 100 Hz) this ratio is little less than 50%, i.e. -3 to -4 dB, depending on tow speed. Above 100 Hz sea noise becomes important and consequently the flow



noise ratio tends to decrease depending on tow speed. At 15 kts sea noise and flow noise remain of the same order, but at lower speeds the ratio gradually decreases. The relatively low values of the flow noise ratio at 6 kts are due to the increased sea state during this experiment. Above 1000 Hz flow noise ratios decrease rapidly. The rise again at 5000 Hz is probably due to spatial aliasing.

The final results of the coherence analysis, flow noise levels as function of frequency, are plotted in *Figure 3c*, in which *Figure 3b* is subtracted from *Figure 3a*. The coherence analysis results are promising. The noise levels at 6, 9, 12 and 15 kts are clearly separated (no longer interfered by different sea states) and tow ship noise/tonals are removed.

So coherence analysis has proven to be a relative simple and successful method to discriminate between sea noise and flow noise. It can be applied to make sensitivity studies on flow noise. For example, the sensitivity of the triplet array to tow speed is approximately 2 dB per knot.

## 6 $k - \omega$ analysis

A linear array of hydrophones provides us with information on the spatial coherence of the noise-field. By analysing this correlation we can determine the distribution of noise power as a function of frequency ( $f$ ), or mathematically more convenient angular frequency ( $\omega$ ), and wavenumber ( $k$ ). These quantities occur after a double FFT, which transfers the array of hydrophone timeseries from the  $(x, t)$  domain to the  $(k, \omega)$  domain. The latter quantities are related to the wave speed of pressure waves ( $c$ ) along the array, which is the ratio of the angular frequency and the longitudinal wavenumber:

$$c = \frac{\omega}{|k|} = \frac{2\pi f}{k \cos \theta}$$

where  $\theta$  is bearing relative to the linear array.

Different noise mechanisms, characterised by different wave speeds, appear as linear “ridges” in the 3D representation of the noise power distribution versus  $\omega$  and  $k$ , i.e. the so-called  $k-\omega$  plot.

Plane sound waves, which are longitudinal pressure waves emitted by distant targets, travel through the array with the sound speed faster than the true sound speed by a factor  $1/\cos\theta$ . This means that the measured sound wave speed increases from 1500 m/s, when the wave is coming from the endfires ( $\theta = 0^\circ$  or  $180^\circ$ ), to infinite values when the waves are coming from broadside ( $\theta = 90^\circ$ ), where the wave reaches all hydrophones at the same time. This leads to the formation of a kind of *acoustic cone* in the  $k-\omega$  plot for wave speeds from  $+1500$  to  $+\infty$  and further from  $-\infty$  to  $-1500$  m/s. Within this cone pressure waves can be acoustic waves (sound) coming from different directions or non-acoustic waves. Outside the cone all waves are non-acoustic (pseudo-sound).

We are interested in the **flow noise levels** on the hydrophones. These can be found by looking at the noise levels outside the acoustic cone. As can be seen in *Figure 4a*, these levels are independent of the wavenumber. This means that noise is uncorrelated from one triplet to the other at these frequencies, which allows compensating for the processing gain of the  $k-\omega$  analysis.

Furthermore  $k-\omega$  analysis teaches us something about the main **causes of flow noise**. Vibrational noise of the array (breathing waves) and direct turbulent noise (advective waves) occur at wave speeds much lower than  $c_0$  and can be distinguished from acoustic noise in the low frequent part of the  $k-\omega$  domain. Due to spatial aliasing the frequency range is limited by an upper value; the design frequency, which is 2070 Hz for the experimental triplet array.



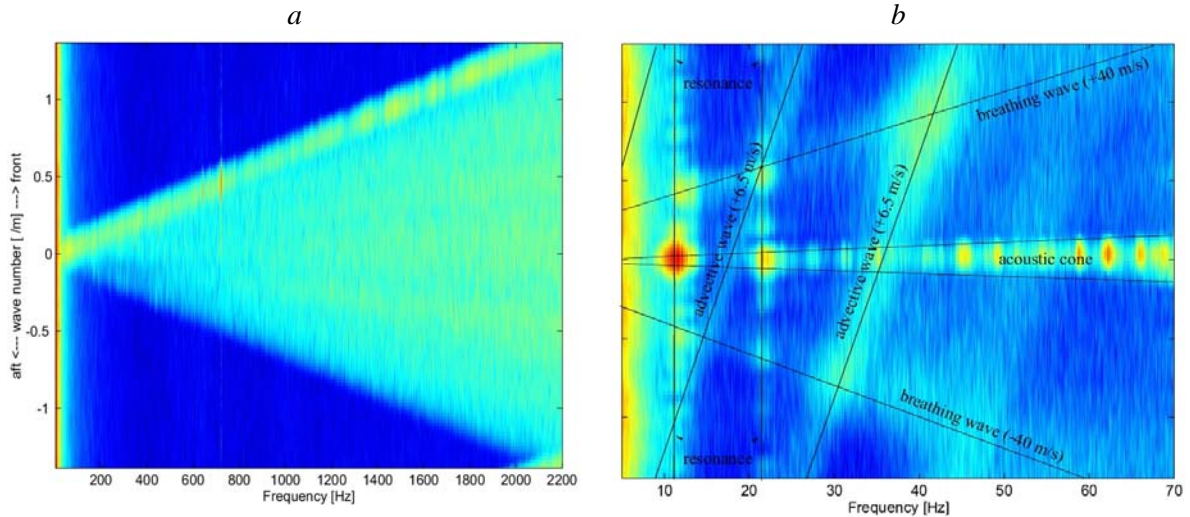


Figure 7  $k$ - $\omega$  analysis for 6 kts and sea state 2 (a) and zoom at LF for 15 kts and sea state 1 (b).

In Figure 7 two typical examples of  $k$ - $\omega$  analysis are worked out, which show contour plots of the noise power density function ( $k$ - $\omega$  plots).

In Figure 7a an experiment at low tow speed (6 kts) and sea state 2 (which is the highest available) is selected. This to emphasise the contrast between sea noise and flow noise. True sound (ambient and tow ship noise) together with pseudo-sound (flow noise) can be found inside the acoustic cone. Outside the acoustic cone the pressure fluctuations are merely due to pseudo-sound (flow noise). Furthermore the tow ship noise coming from forward direction can be recognised by this analysis. Clearly visible is the Tydeman spectrum at wave speed little over 1500 m/s. The exact value corresponds to an incidence angle of about  $20^\circ$ , which is in agreement with the used cable scope (1000 m) and tow speed (6 kts).

In Figure 7b a zoom on lower frequencies of a  $k$ - $\omega$  plot is shown for the experiment conducted at a relatively high tow speed of 15 kts. In this plot the sources of flow noise, as shown in Figure 2, become visible. Phenomena as breathing and advective waves, show up as ridges with a constant wave speed. Clearly visible are three ridges corresponding to two types of waves: two breathing waves with speeds of approximately  $\pm 40$  m/s, and an (aliased) advective wave with a speed of approximately +6.5 m/s, which is in accordance to theory about 90% of the tow speed. Other wave types (extensional waves, elastic waves) are not regularly found in the triplet array. Furthermore a (electronic?) resonance is visible at 12 Hz and its higher harmonics at 24 and 48 Hz.

## 7 Conclusions

Considering the studied methods to analyse flow noise data the following remarks can be made:

- Spectral analysis (Chapter 4) is not to be trusted. The method is simple and straightforward and therefore attractive to people who want fast results. However, the results depend on too many external factors and sometimes differ considerable from coherence analysis and  $k$ - $\omega$  analysis, which on their turn are very consistent.
- Coherence analysis (Chapter 5) is also relatively simple and proofs successful in discriminating flow noise from sea noise. However, there are doubts about the applicability at low frequencies. The advantage of the method is that it is very fast and therefore suitable for comprehensive parameter studies and for future real-time applications in adaptive beamformers.
- $k$ - $\omega$  analysis (Chapter 6) provides both qualitative and quantitative results, so that the levels and the causes of flow noise can be isolated.

In Figure 8 the flow noise levels as a result of coherence analysis are compared to Knudsen curves for sea state 0, 1, 3 and 6, respectively. Only at very low frequencies flow noise is limiting. The

flow noise levels in the active band are always lower than moderate sea states, i.e. sea state 1-2. For 6 kts flow noise is negligible, for 9 and 12 kts flow noise is in between sea state 0 and 1, and for 15 kts the flow noise level is little higher than sea state 1. The increase of flow noise with tow speed is about 2 dB per knot.

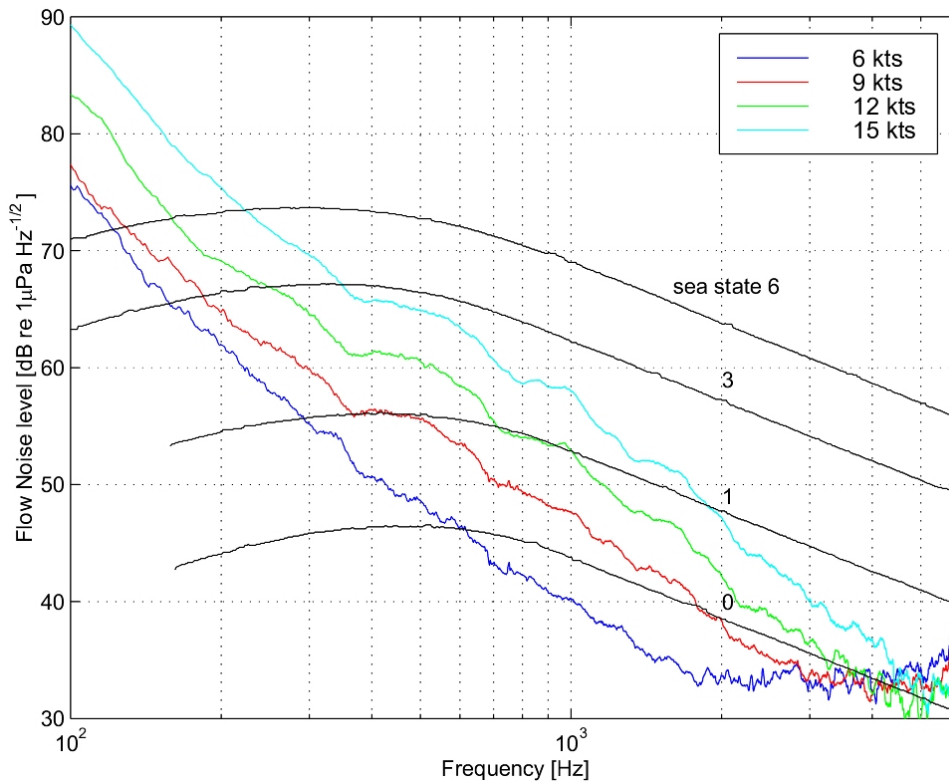


Figure 8: Comparison of flow noise levels to Knudsen curves for sea state 0,1,3,6

## References

- [1] G.W.M. van Mierlo, S.P. Beerens, R. Been, Y.Doisy & E.Trouvé, Port/Starboard discrimination on hydrophone triplets in active and passive towed arrays, Proceedings of UDT, 176-181, 1997.
- [2] S.P. Beerens, S.P. van IJsselmuide, C. Volwerk, Y.Doisy & E.Trouvé, Flow noise analysis of towed sonar arrays, Proceedings of UDT, 1999.
- [3] W.K. Blake, Mechanics of Flow-Induced Sound and Vibration I+II, Academic Press, 1986.
- [4] G.M Corcos, The resolution of turbulent pressure at the wall of a boundary layer, J.Sound Vib. 6 (1), 1967.
- [5] R.J. Urick, Principles of underwater sound, McGraw Hill, 1983 (third edition).